A LETTERS JOURNAL EXPLORING THE FRONTIERS OF PHYSICS

OFFPRINT

New type of equilibrium distribution for a system of charges in a spherically symmetric electric field

GABRIELA A. CASAS, FERNANDO D. NOBRE and EVALDO M. F. CURADO

EPL, **126** (2019) 10005

epl

A Letters Journal Exploring the Frontiers of Physics

AN INVITATION TO SUBMIT YOUR WORK

epljournal.org

The Editorial Board invites you to submit your Letters to EPL

Choose EPL, and you'll be published alongside original, innovative Letters in all areas of physics. The broad scope of the journal means your work will be read by researchers in a variety of fields; from condensed matter, to statistical physics, plasma and fusion sciences, astrophysics, and more.

Not only that, but your work will be accessible immediately in over 3,300 institutions worldwide. And thanks to EPL's green open access policy you can make it available to everyone on your institutional repository after just 12 months.

Run by active scientists, for scientists

Your work will be read by a member of our active and international Editorial Board, led by Bart Van Tiggelen. Plus, any profits made by EPL go back into the societies that own it, meaning your work will support outreach, education, and innovation in physics worldwide.

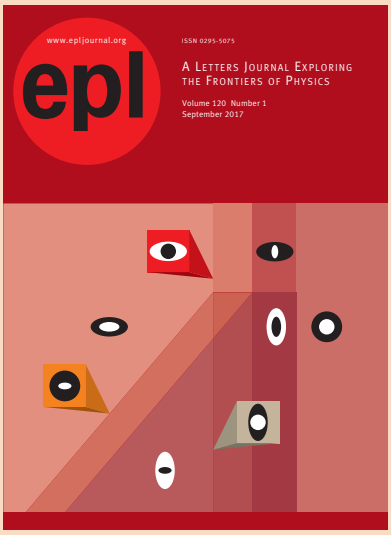

OVER

638,000

full-text downloads in 2017

Average submission to online publication

100 DAYS

21,500

citations in 2016

We greatly appreciate the efficient, professional and rapid processing of our paper by your team.

Cong Lin
Shanghai University

Four good reasons to publish with EPL

1. **International reach** – more than 3,300 institutions have access to EPL globally, enabling your work to be read by your peers in more than 90 countries.

2. **Exceptional peer review** – your paper will be handled by one of the 60+ co-editors, who are experts in their fields. They oversee the entire peer-review process, from selection of the referees to making all final acceptance decisions.

3. **Fast publication** – you will receive a quick and efficient service; the median time from submission to acceptance is 75 days, with an additional 20 days from acceptance to online publication.

4. **Green and gold open access** – your Letter in EPL will be published on a green open access basis. If you are required to publish using gold open access, we also offer this service for a one-off author payment. The Article Processing Charge (APC) is currently €1,400.

Details on preparing, submitting and tracking the progress of your manuscript from submission to acceptance are available on the EPL submission website, **epletters.net**.

If you would like further information about our author service or EPL in general, please visit **epljournal.org** or e-mail us at **info@epljournal.org**.

EPL is published in partnership with:

European Physical Society

Società Italiana di Fisica

EDP Sciences

IOP Publishing

A Letters Journal Exploring the Frontiers of Physics

April 2019

EPL, **126** (2019) 10005 www.epljournal.org
doi: 10.1209/0295-5075/126/10005

New type of equilibrium distribution for a system of charges in a spherically symmetric electric field

Gabriela A. Casas[1], Fernando D. Nobre[1,2] and Evaldo M. F. Curado[1,2]

[1] *Centro Brasileiro de Pesquisas Físicas - Rua Dr. Xavier Sigaud 150, 22290-180 Rio de Janeiro, Brazil*
[2] *National Institute of Science and Technology for Complex Systems - Rua Dr. Xavier Sigaud 150, 22290-180 Rio de Janeiro, Brazil*

received 5 February 2019; accepted in final form 9 April 2019
published online 21 May 2019

PACS 05.40.Fb – Random walks and Levy flights
PACS 05.70.Ce – Thermodynamic functions and equations of state
PACS 05.90.+m – Other topics in statistical physics, thermodynamics, and nonlinear dynamical systems

Abstract – A system of N mobile negatively charged particles moving in a neutral and dissipative medium, under a confining electric field produced by a spherical-capacitor apparatus, is studied. The equations of motion are approximated to the continuous limit leading to a nonlinear Fokker-Planck equation; these analytical results are supported by molecular-dynamics simulations. The definitively non-Yukawa equilibrium position distribution, which emerges from first principles, is expressed in terms of a q-exponential function. The present work opens the door to new experiments in a system with long-range repulsive interactions, indicated herein as a potential candidate for nonextensive statistical mechanics.

The elegant connection between statistical mechanics and thermodynamics represents a significant scientific achievement towards an appropriate theoretical description of a system of interacting particles [1,2]. Such a link of the microscopic and macroscopic worlds usually occurs through the entropy concept, so that its knowledge becomes a crucial step in this pathway. Additionally, the association of the entropy with dynamics represents a remarkable result of nonequilibrium statistical mechanics and it appears through the following procedures: i) the statistical entropy may be extremized under appropriate constraints, yielding an equilibrium probability that coincides with the stationary-state distribution of a time-evolution equation for the probabilities (*e.g.*, a Fokker-Planck equation [3]); ii) an H-theorem, which may be proven by considering the statistical entropy and an equation for the time evolution of the probabilities [1–3].

Depending on the type of interactions and/or correlations among constituents, the outstanding framework of Boltzmann-Gibbs (BG) equilibrium statistical mechanics may not apply; particularly the classification of all thermodynamic quantities in two classes, namely, intensive and extensive, may break down [1]. For N-particle systems characterized by long-range interactions, some fundamental quantities, *e.g.*, internal energy and temperature, may not remain extensive and intensive, respectively, presenting a nonlinear dependence with N. In order to fulfill the thermodynamical Legendre structure, in these anomalous cases one ends up with nonextensive quantities (*e.g.*, the thermodynamic potentials), extensive ones (*e.g.*, number of particles and entropy), as well as an additional category (*e.g.*, the scaled temperature), which represents quantities that do not remain intensive. Lately, many systems in nature, specially those within the realm of complex systems, have presented such anomalous behavior, leading to the development of the area of nonextensive statistical mechanics [4]. This framework is based on the proposal of a generalized entropic form S_q, which depends on a parameter q ($q \in \Re$), such that the BG entropy is recovered in the limit $q \to 1$. Connections among entropies and dynamics were extended for generalized entropic forms by many authors (see, *e.g.*, refs. [5–11]), mostly by making use of nonlinear Fokker-Planck equations (NLFPEs).

Recently, systems characterized by the entropy S_q (with $q \neq 1$) have exhibited a consistent thermodynamic framework; as an example, one could mention works on the equilibrium state of interacting vortices, usually considered as a model for type-II superconductors [12–17]. An effective-temperature θ was introduced, shown to be proportional to the density of vortices, a quantity that may be varied

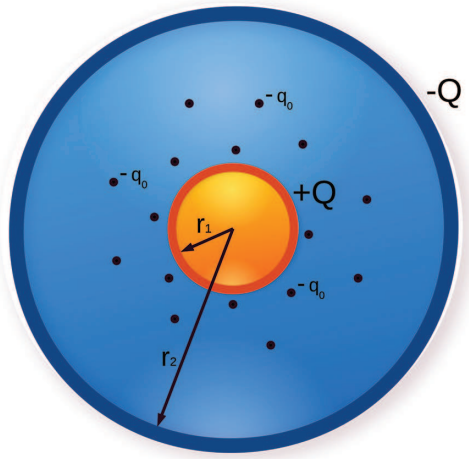

Fig. 1: The system investigated consists of N negative charges $-q_0$ ($q_0 > 0$), inside a spherical region, between two concentrical conducting shells of radius r_1 and r_2 ($r_2 > r_1$). This region is filled with a neutral fluid that produces friction, so that the particles move under overdamped motion. The shells are charged (total charges $\pm Q$), leading to a spherically symmetric electric field $\vec{E}$ pointing outwards.

experimentally [18]. In this approach, the temperature θ appeared as the parameter thermodynamically conjugated to the entropy S_2 [12].

Systems of charges are known as exceptional in what concerns BG statistical mechanics, being characterized by properties that may depend on the shape of the sample; in this sense, the thermodynamic limit becomes troublesome [1]. Several examples where Coulomb interactions are present have shown inconsistencies with the standard statistical-mechanics theory (see, *e.g.*, refs. [19–31]). In the present work we illustrate some of these difficulties by considering a physical system (illustrated in fig. 1) formed by N similar colloidal particles, each presenting an electric charge $-q_0$ ($q_0 > 0$), and placed inside a spherical-capacitor apparatus, built by two concentrical spherical conducting shells of radius r_1 and r_2 ($r_2 > r_1$). The inner shell presents a total charge $+Q$, whereas the outer one has charge $-Q$, producing a spherically symmetric electric field $\mathbf{E} = (Q/r^2)\hat{\mathbf{r}}$ ($r_1 \leq r \leq r_2$) (we adopt Gaussian units [32]). We also assume that the region between the two shells is filled with a neutral fluid, so that these charged spheres (with typical diameters of the order of 100 nm) move under friction (friction coefficient μ), and that inertial effects can be neglected, *i.e.*, an overdamped motion. In this way, the equation of motion of a particle i is given by [33–35]

$$\mu \mathbf{v}_i = \mathbf{F}_i^{\mathrm{pp}} + \mathbf{F}_i^{(\mathbf{E})} \qquad (i = 1, 2, \ldots, N), \tag{1}$$

where $\mathbf{v}_i$ represents its velocity, $\mu\mathbf{v}_i$ stands for the friction contribution, and the forces on the right-hand side are both radially symmetric, with $\mathbf{F}^{(\mathbf{E})} = (-q_0 Q/r^2)\hat{\mathbf{r}}$ being due to the electric field $\mathbf{E}$ on particle i.

Moreover, $\mathbf{F}_i^{\mathrm{pp}}$ results from the Coulomb particle-particle interactions,

$$\mathbf{F}_i^{\mathrm{pp}} = \sum_{j \neq i} \frac{q_0^2}{r_{ij}^2}\, \hat{\mathbf{r}}_{ij}, \tag{2}$$

and as usual, $r_{ij} = |\mathbf{r}_i - \mathbf{r}_j|$ stands for the distance between particles i and j, whereas $\hat{\mathbf{r}}_{ij} = (\mathbf{r}_i - \mathbf{r}_j)/r_{ij}$ is a vector defined along the axis of each pair of particles.

Therefore, if one considers all charges near the inner shell at an initial time, the particle-particle repulsive forces push them outwards, whereas the electric field $\mathbf{E}$ acts on the opposite direction; for sufficiently long times one expects to attain an electrostatic equilibrium. One of the aims of this work is the derivation of a mesoscopic equation for the time evolution of the density of particles $\rho(\mathbf{r}, t)$, at time t and position $\mathbf{r}$. Based on the conservation of the total number of particles, $\rho(\mathbf{r}, t)$ should follow the continuity equation,

$$\frac{\partial \rho(\mathbf{r}, t)}{\partial t} + \nabla \cdot \mathbf{J} = 0, \tag{3}$$

with $\mathbf{J} = \rho\mathbf{v}$ representing the current density. Hence, one may write the force $\mathbf{F}^{\mathrm{pp}}$ on a particle located at $\mathbf{r}$ as

$$\mathbf{F}^{\mathrm{pp}} = \int \mathrm{d}^3 r' \rho(\mathbf{r} + \mathbf{r}', t) \frac{q_0^2}{r'^2} \hat{\mathbf{r}}', \tag{4}$$

where we have replaced $r_{ij} \to r'$. Under physical conditions where the density varies smoothly around the point $\mathbf{r}$, one may expand $\rho(\mathbf{r} + \mathbf{r}', t) \approx \rho(\mathbf{r}, t) + \mathbf{r}' \cdot \nabla \rho(\mathbf{r}', t)|_{\mathbf{r}'=\mathbf{r}}$. Substituting this expansion in eq. (4) one gets that the integral over $\rho(\mathbf{r}, t)$ vanishes, due to symmetry; moreover, since $\mathbf{F}^{\mathrm{pp}}$ and $\nabla\rho(\mathbf{r}, t)$ are antiparallel, one obtains $\mathbf{F}^{\mathrm{pp}} \approx -a\nabla\rho(\mathbf{r}, t)$, with

$$a = \int \mathrm{d}^3 r' \frac{q_0^2}{r'} = 4\pi q_0^2 \int_0^{r_2 - r_1} \mathrm{d}r' r' = 2\pi q_0^2 (r_2 - r_1)^2. \tag{5}$$

Due to the long-range character of the interactions, the integral above diverges in the limit $r_2 \to \infty$, in contrast with previous short-range-interaction approaches [33–35]. The quantity a must be finite, since it will appear in the diffusion coefficient of a NLFPE, to be shown next.

Then, one may substitute these results into eq. (3) and use eq. (1) to get

$$\mu \frac{\partial \rho(\mathbf{r}, t)}{\partial t} = \nabla \cdot \left\{ \rho(\mathbf{r}, t) \left[a \nabla \rho(\mathbf{r}, t) + \frac{\mathrm{d}\phi(r)}{\mathrm{d}r} \hat{\mathbf{r}} \right] \right\}, \tag{6}$$

where we introduced an effective potential energy $\phi(r)$ (associated with the electric field $\mathbf{E}$ and screening effects), to be discussed next. Since the radial direction is the relevant one, we restrict to the variable r,

$$\mu \frac{\partial \rho(r, t)}{\partial t} = \frac{1}{r^2} \frac{\partial}{\partial r} \left\{ r^2 \rho(r, t) \frac{\mathrm{d}\phi(r)}{\mathrm{d}r} \right\} + \frac{a}{r^2} \frac{\partial}{\partial r} \left\{ r^2 \rho(r, t) \frac{\partial \rho(r, t)}{\partial r} \right\}. \tag{7}$$

It should be mentioned that although the physical system illustrated in fig. 1 is different from an electrolyte, where various charged ions with opposite signs are present, herein screening effects also play an important role [36]. In an electrolyte, considering the particle-particle interactions within a mean-field approximation (known as Debye-Hückel theory), the electrostatic potential of a charge at a distance r from the origin gets modified by an exponential factor $\exp(-\beta r)$, with a screening length β^{-1}. This effect, due to other charges, appears also in nuclear physics and the corresponding electrostatic potential is known as Yukawa potential [32], which is expressed herein in the following form:

$$\phi_1(r) = \frac{B_0}{r}\exp[-\beta(r-r_1)] \qquad (r_1 \le r \le r_2), \qquad (8)$$

where B_0 is a constant and the notation $\phi_1(r)$ will become clear below. In the present problem, the actual form of the effective potential energy $\phi(r)$ that appears in eq. (7) is not straightforward to calculate analytically, and it will be determined through fittings of the numerical data; indeed, we will verify that the Yukawa form above applies only close to the inner radius r_1.

The stationary-state solution of eq. (7) is obtained by setting its right-hand side equal to zero; in fact, this state corresponds to an electrostatic equilibrium, in which all forces on each particle cancel, and the corresponding density of particles will be called $\rho_{\rm eq}(r)$. Hence, considering the electrostatic equilibrium in eq. (7),

$$\rho_{\rm eq}(r) = -\frac{\phi(r)}{a} + C_1. \qquad (9)$$

For simplicity we set $\rho_{\rm eq}(r_2) = 0$, which will affect only the additive constant in the resulting $\rho_{\rm eq}(r)$; the validity of this condition is supported by the numerical simulations, where $[\rho_{\rm eq}(r_2)/\rho_{\rm eq}(r_1)] < 10^{-6}$ will be found, for typically, $r_2 - r_1 \sim 10^3$. Therefore,

$$\rho_{\rm eq}(r) = \frac{\rho_{\rm eq}(r_1)}{\phi(r_1)-\phi(r_2)}[\phi(r)-\phi(r_2)]. \qquad (10)$$

We carried molecular-dynamics simulations by integrating eqs. (1) for given parameters of the system shown in fig. 1. All simulations started with N charged particles around the inner shell, so that their repulsive forces push them away from the inner shell. After a sufficiently long time, one approaches the electrostatic equilibrium, on which we constructed histograms to obtain $\rho_{\rm eq}(r)$. In this numerical procedure we considered a time step $\delta t = 10^{-3}$, so that each unit of (physical) time corresponds to 10^3 integrations of eqs. (1); a typical time used for approaching the equilibrium state was $t_{\rm eq} = 1000$, *i.e.*, 10^6 integrations of the equations of motion. Due to the long-range character of the interactions, one must have an appropriate balance between the value of Q and the choices of N and q_0, for fixed values of r_1 and r_2. One should remind that to be consistent with the approximations used, the equilibrium density $\rho_{\rm eq}(r)$ should be continuous; we verified that for certain choices of the parameters this requirement is not necessarily fulfilled. Indeed, for systems of charges one may find equilibrium configurations composed by separated aggregates of particles [37]; these cases may lead to discontinuities in $\rho_{\rm eq}(r)$.

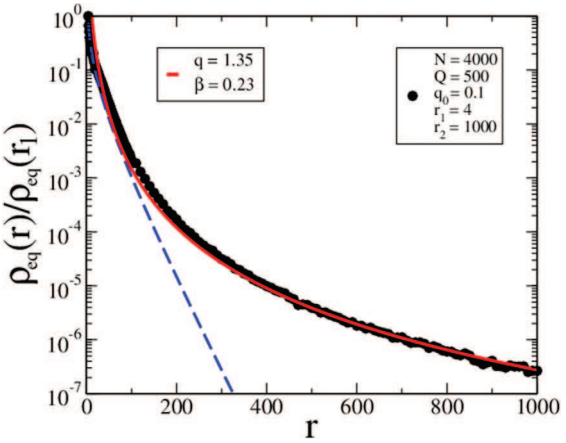

Fig. 2: Equilibrium density $\rho_{\rm eq}(r)$ is plotted *vs.* r in a log-linear representation, for typical values of the relevant parameters. The symbols (black circles) are results from simulations, whereas the full red line represents the fitting proposal of eq. (11). An illustrative Yukawa potential (cf. eq. (8)) is represented by the dashed blue line. Lengths and charges are represented in units of a characteristic length $l(r_1, r_2)$ and a typical charge $\tilde{q}$, respectively (see text).

In fig. 2 we present numerical results for $\rho_{\rm eq}(r)$, together with two fitting proposals for $\phi(r)$ (substituted in eq. (10)), namely, the Yukawa form of eq. (8) (dashed blue line), and the modified one (full red line),

$$\begin{aligned}\phi_q(r) &= \frac{B_0}{r}\exp_q[-\beta(r-r_1)] \\ &= \frac{B_0}{r}[1-(1-q)\beta(r-r_1)]_+^{1/(1-q)}, \end{aligned} \qquad (11)$$

where $\exp_q(x) = [1+(1-q)x]_+^{1/(1-q)}$, with $[y]_+ = y$, for $y > 0$, zero otherwise, so that $\lim_{q\to 1}\phi_q(r) = \phi_1(r)$ [4]. Clearly, the first proposal appears to be good only for small values of r, whereas the second one fits well the whole set of data. It should be mentioned that the form in eq. (11) has been considered previously, for systems characterized by Coulomb interactions, more precisely, in plasmas and colloidal suspensions [22–31]. In the present case, the modification of the electrostatic potential energy of a charged particle at a distance r is attributed to screening effects caused by other charges, at distances $r' < r$, which diminish gradually the intensity of the electric field acting on this charge. In this way, the potential energy $\phi(r)$ presents its maximum (unscreened) value at $r = r_1$, decreasing for increasing values of r, with the screening effects leading to eq. (11).

The parameter β (cf. eqs. (8) and (11)) presents dimensions $(\text{length})^{-1}$; assuming that it depends only on

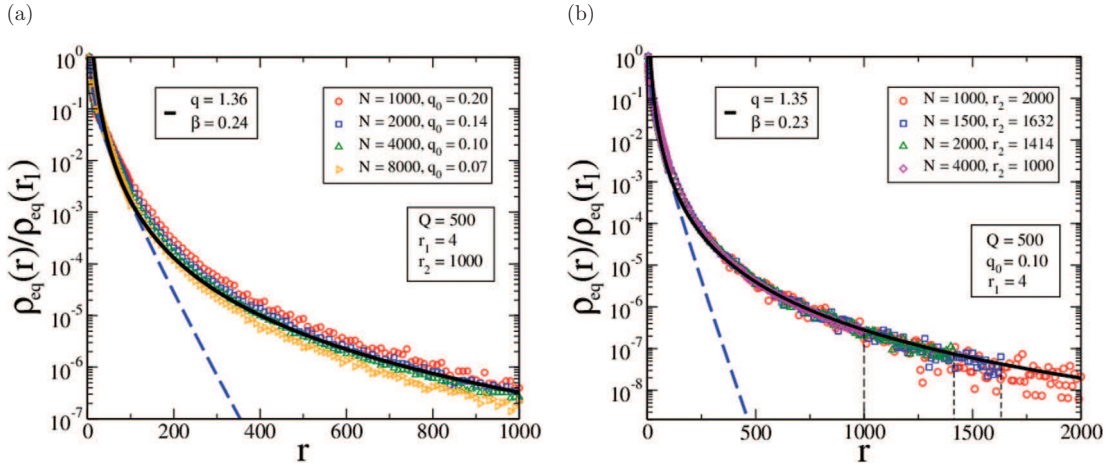

Fig. 3: Equilibrium densities $\rho_{\rm eq}(r)$ are plotted *vs.* r in log-linear representations, by varying some relevant parameters of the system (with r_1 fixed), but keeping the diffusion coefficient of eq. (20) typically unchanged, *i.e.*, $Nq_0^2r_2^2 = \text{const}$ (the numerical data above correspond to $Nq_0^2r_2^2 = 4.0 \times 10^7$). (a) Plots for r_2 fixed and several choices for N and q_0. (b) Plots for q_0 fixed and several choices for N and r_2; the vertical dashed lines indicate the values of r_2 considered. The symbols are results from molecular-dynamics simulations, whereas the full lines represent the fitting proposal of eq. (11). In both cases, illustrative Yukawa potentials (cf. eq. (8)) are represented by dashed blue lines. Lengths and charges are represented in units of a characteristic length $l(r_1, r_2)$ and a typical charge $\tilde{q}$, respectively (see text).

the two radii, one may introduce a length scale $l(r_1, r_2) \equiv b[\beta(r_1, r_2)]^{-1}$, where b stands for a dimensionless proportionality constant. The knowledge of a precise form for $l(r_1, r_2)$ requires further extensive simulations, being out of the scope of the present investigation; however, based on the present numerical analysis, we propose a limiting behavior of $[\beta(r_1, r_2)]$ for $r_2 \gg r_1$. Moreover, to compare analytical and numerical results, we also introduce a unit of charge $\tilde{q}$; therefore, lengths and charges are herein expressed in units of $l(r_1, r_2)$ and $\tilde{q}$, respectively[1].

As mentioned above, by varying significantly one of the parameters (N, Q, q_0, r_1, r_2) separately, one could get unbalanced configurations. Nevertheless, there are particular combinations of these parameters that may be fixed to yield invariant density profiles. This aspect is illustrated in fig. 3, where we present numerical data obtained by changing significantly the relevant parameters (with respect to those of fig. 2), but keeping $Nq_0^2r_2^2 = \text{const}$; as will be shown next, this product appears in the diffusion coefficient of the NLFPE. In fig. 3(a) we show results for $r_2 = 10^3$ and several choices of N and q_0, whereas in fig. 3(b) we take $q_0 = 0.10$, with N and r_2 varying; in all cases the equilibrium density $\rho_{\rm eq}(r)$ remains unchanged (within the error bars), expressed in terms of the proposal of eq. (11) with $q = 1.35 \pm 0.01$ and $\beta = 0.24 \pm 0.01$. We verified that these results are robust under slight variations (up to 10%, typically) of one of the parameters (N, Q, q_0, r_1, r_2). As will be seen later on, the product $Nq_0^2r_2^2$ appears in an effective-temperature definition, for $r_2 \gg r_1$; hence, all plots shown in fig. 3 correspond to the same effective temperature.

[1]In an experimental apparatus one could expect $l \approx 0.1\,\text{cm}$ and $\tilde{q} \approx 10^3\text{e} = 4.8 \times 10^{-7}\,\text{esu}$.

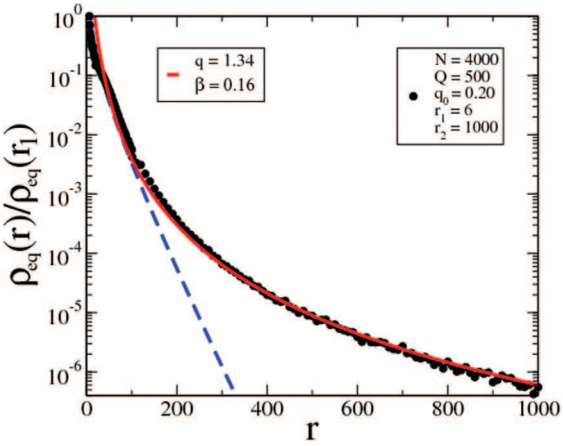

Fig. 4: Equilibrium density $\rho_{\rm eq}(r)$ is plotted *vs.* r in log-linear representation, for a value of the inner radius different from the one used in figs. 2 and 3. As discussed in the text, the value of q_0 has to be varied accordingly. The symbols are results from molecular-dynamics simulations, whereas the full line represents the fitting proposal of eq. (11). An illustrative Yukawa potential (cf. eq. (8)) is represented by the dashed blue line. Lengths and charges are represented in units of a characteristic length $l(r_1, r_2)$ and a typical charge $\tilde{q}$, respectively (see text).

In fig. 4 we present $\rho_{\rm eq}(r)$ for $q_0 = 0.20$ and an inner radius $r_1 = 6$, keeping other parameters fixed with respect to those used in fig. 2. One should notice that by increasing the inner radius, the average distance between particles will increase at the initial configuration, so that the contribution due to the electric field $\mathbf{E}$ will prevail over the repulsive particle-particle interactions; as a consequence, the dynamics becomes quite trivial, with most particles remaining near the inner shell. For this reason, the value

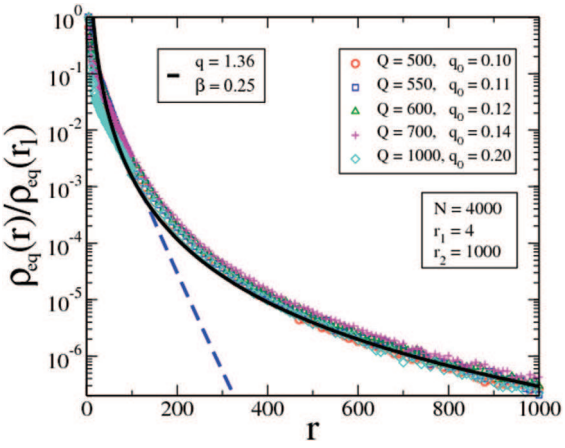

Fig. 5: Equilibrium density $\rho_{\rm eq}(r)$ is plotted *vs.* r in log-linear representation, by varying the values of Q and q_0, but keeping the ratio $Q/q_0 = \text{const}$ (the numerical data above correspond to $Q/q_0 = 5.0 \times 10^3$). The symbols are results from molecular-dynamics simulations, whereas the full line represents the fitting proposal of eq. (11). An illustrative Yukawa potential (cf. eq. (8)) is represented by the dashed blue line. Lengths and charges are represented in units of a characteristic length $l(r_1, r_2)$ and a typical charge $\tilde{q}$, respectively (see text).

of q_0 needs to be increased as well, in such a way to approach an equilibrium state with a continuous equilibrium density $\rho_{\rm eq}(r)$, as shown in fig. 4. In this case, the fitting proposal of eq. (11) applies, with the same value of q used in figs. 2 and 3, within the error bars ($q = 1.35 \pm 0.01$). However, the value of β varied significantly, estimated as $\beta = 0.16 \pm 0.01$, showing its direct dependence on the choice of the inner radius r_1. In fact, the results of figs. 2–4 indicate that $[\beta(r_1, r_2)]^{-1} \approx r_1$, for $r_2 \gg r_1$, suggesting that r_1 is approximately the typical length scale of the system. Furthermore, these plots show that, contrary to β, the value of q is not sensitive to variations in r_1; this appears to be a natural result, since one expects q to affect significantly the form of the distribution, and particularly, its behavior for large values of r.

At the equilibrium state all forces on each particle cancel, *i.e.*, the repulsive particle-particle contribution of eq. (2) (proportional to q_0^2) equals the one due to the electric field (proportional to $q_0 Q$); as a consequence, the relation $Q/q_0 = \text{const}$ is expected to hold. In order to show the consistency of our simulations with such an equilibrium state, in fig. 5 we present numerical results by varying the values of Q and q_0, but keeping the ratio $Q/q_0 = \text{const}$ (other parameters are kept fixed to those values of fig. 2). One verifies a reasonable collapse of all data, so that the fitting proposal of eq. (11) applies with the same values of q and β considered in figs. 2 and 3, within the error bars. Hence, all curves presented in fig. 5 correspond to the same electrostatic equilibrium condition.

By means of the characteristic length $l(r_1, r_2)$, we define a dimensionless probability $P(r,t) \equiv l^3 \rho(r,t)/N$, so that the condition $4\pi \int_{r_1}^{r_2} {\rm d}r\ r^2 \rho(r,t) = N$ yields the normalization constraint,

$$\frac{4\pi}{l^3} \int_{r_1}^{r_2} {\rm d}r\ r^2 P(r,t) = 1. \tag{12}$$

Therefore, the following NLFPE results:

$$\mu \frac{\partial P(r,t)}{\partial t} = \frac{1}{r^2} \frac{\partial}{\partial r} \left\{ r^2 P(r,t) \frac{{\rm d}\phi(r)}{{\rm d}r} \right\} + \frac{2D}{r^2} \frac{\partial}{\partial r} \left\{ r^2 P(r,t) \frac{\partial P(r,t)}{\partial r} \right\}, \tag{13}$$

where we have introduced $2D = Na/l^3$. The above equation may still be written in the form of a continuity equation,

$$\mu \frac{\partial P(r,t)}{\partial t} = -\frac{1}{r^2} \frac{\partial [r^2 J(r,t)]}{\partial r}, \tag{14}$$

with the boundary conditions,

$$J(r,t)|_{r=r_1} = J(r,t)|_{r=r_2} = 0 \qquad (\forall t), \tag{15}$$

that ensure the conservation of the total number of particles (and consequently, of the probability $P(r,t)$) in the region $r_1 < r < r_2$, for all times.

Next, we will use the NLFPE of eq. (13) to prove an H-theorem; for this, we consider the general entropic form [10,11]

$$S[P(\mathbf{r},t)] = \frac{k}{l^3} \int {\rm d}^3 r g[P] = \frac{4\pi k}{l^3} \int_{r_1}^{r_2} {\rm d}r\ r^2 g[P(r,t)],$$
$$g(0) = g(1) = 0, \qquad \frac{{\rm d}^2 g[P]}{{\rm d}P^2} \leq 0, \tag{16}$$

where k is a positive constant with entropy dimensions and $g[P]$ should be at least twice differentiable. The present H-theorem concerns a well-defined sign for the time derivative of the free-energy functional [10,11]

$$F = U - \theta S, \qquad U = \frac{4\pi}{l^3} \int_{r_1}^{r_2} {\rm d}r\ r^2 \phi(r) P(r,t), \tag{17}$$

where θ represents a positive parameter with dimensions of temperature. Hence, considering the time derivative of the functional above, and using eq. (14), one obtains

$$\frac{\partial F}{\partial t} = -\frac{4\pi}{\mu l^3} \int_{r_1}^{r_2} {\rm d}r \left(\phi(r) - k\theta \frac{{\rm d}g[P]}{{\rm d}P} \right) \frac{\partial [r^2 J(r,t)]}{\partial r} \tag{18}$$

so that integrating by parts and using the boundary conditions in eq. (15), one gets that

$$\frac{\partial F}{\partial t} = -\frac{4\pi}{\mu l^3} \int_{r_1}^{r_2} {\rm d}r\ r^2 P \left(-\frac{{\rm d}\phi(r)}{{\rm d}r} - 2D \frac{\partial P}{\partial r} \right) \times \left(-\frac{{\rm d}\phi(r)}{{\rm d}r} + k\theta \frac{{\rm d}^2 g}{{\rm d}P^2} \frac{\partial P}{\partial r} \right). \tag{19}$$

Following previous works on physical applications of NLFPEs [12–17], we define an effective temperature θ,

$$D \equiv k\theta = \frac{\pi N q_0^2 \ (r_2 - r_1)^2}{l^3}, \tag{20}$$

where we have used $D = Na/2l^3$, together with eq. (5). Herein, we remind that the radius r_2 should be kept finite, in order to fulfill the requirement of a finite diffusion coefficient and consequently, a finite effective temperature θ. As mentioned before, the numerical results shown in fig. 3, which keep $D = \text{const}$, reinforce further the coarse-graining procedure that led to the NLFPE of eq. (13). Now, imposing in eq. (19)

$$\frac{\mathrm{d}^2 g[P]}{\mathrm{d}P^2} = -2, \tag{21}$$

one ends up with the H-theorem expressed in the form

$$\frac{\partial F}{\partial t} = -\frac{4\pi}{\mu l^3} \int_{r_1}^{r_2} \mathrm{d}r \ r^2 P \left(-\frac{\mathrm{d}\phi(r)}{\mathrm{d}r} - 2D \frac{\partial P}{\partial r} \right)^2 \leq 0. \tag{22}$$

Notice that the numerical results shown in fig. 3 (for which $r_2 \gg r_1$, keeping D essentially unchanged) reinforce the approximations that led to the NLFPE of eq. (13). In what concerns the effective-temperature defined above, it is important to stress that: i) a finite radius r_2 becomes a necessary condition; ii) the relation $\theta \approx N q_0^2 r_2^2 / l^3$ shows that θ may be interpreted in terms of a linear density of particles. This result is similar to the effective-temperature concept introduced recently for a system of interacting vortices, used as a model for type-II superconductors [12–17]; experimentally, one expects that this quantity may be varied continuously [18].

A direct consequence of eq. (21), imposed to satisfy the H-theorem, is the corresponding associated entropic form [10,11]; integrating eq. (21) twice, and using the conditions $g(0) = g(1) = 0$, one obtains $g[P] = P - P^2$. Therefore, the entropy of eq. (16) becomes

$$S[P] = k \left[1 - \frac{4\pi}{l^3} \int_{r_1}^{r_2} \mathrm{d}r \ r^2 P^2(r,t) \right], \tag{23}$$

which corresponds to Tsallis entropy S_q with $q = 2$ [4].

Let us now extremize the entropy above under the constraints of normalization (eq. (12)) and internal energy of of eq. (17). Thus, we introduce the functional [1],

$$\mathcal{I}[P] = \frac{S[P]}{k} + \alpha \left(1 - \frac{4\pi}{l^3} \int_{r_1}^{r_2} \mathrm{d}r \ r^2 P(r,t) \right) + \gamma \left(U - \frac{4\pi}{l^3} \int_{r_1}^{r_2} \mathrm{d}r \ r^2 \phi(r) P(r,t) \right), \tag{24}$$

where α and γ are Lagrange multipliers. Using $g[P] = P - P^2$, the extremization of $\mathcal{I}[P]$ yields the equation for the equilibrium distribution $P_{\mathrm{eq}}(r)$,

$$1 - 2P_{\mathrm{eq}} - \alpha - \gamma\phi(r) = 0. \tag{25}$$

Now, multiplying the above equation by N/l^3, one gets

$$\rho_{\mathrm{eq}}(r) = \frac{N\gamma}{2l^3} \left[-\phi(r) + \tilde{C}_1 \right], \tag{26}$$

which coincides with eq. (9) (apart from an additive constant), by choosing the Lagrange multiplier $\gamma = 2l^3/(Na)$, corresponding to $\gamma = 1/D = (k\theta)^{-1}$. Therefore, we have shown that the entropic form that satisfies the H-theorem may be extremized to yield an equilibrium distribution that coincides with the stationary-state solution of the corresponding NLFPE.

To summarize, we have studied a system of charged particles inside a spherically symmetric medium. The equations of motion were approximated to the continuous limit leading to a nonlinear Fokker-Planck equation, where the diffusion coefficient is well defined only for a finite system. The analytical results are supported by molecular-dynamics numerical simulations. We have shown that the resulting nonlinear Fokker-Planck equation is associated with an entropic functional of Tsallis type, S_q with $q = 2$, corroborating recent investigations carried for systems of particles interacting repulsively through short-range forces, for which the coarse-graining method could be applied, in principle, for an infinite volume [34,35]. Interestingly, the equilibrium distribution is expressed in terms of a q-deformed Yukawa potential, in the context of nonextensive statistical mechanics, where a q-exponential ($q \approx 1.35$) appears. Although this latter index is not obviously connected to the entropic index $q = 2$, we can not exclude the possibility of a relation between them. The present proposal opens the possibility of experimental verifications for a physical system characterized by long-range particle-particle interactions, described by nonextensive statistical mechanics.

* * *

The authors thank C. Tsallis for fruitful conversations. Partial financial support from CNPq, CAPES, and FAPERJ (Brazilian funding agencies) is acknowledged.

REFERENCES

[1] Balian R., *From Microphysics to Macrophysics*, Vols. **I** and **II** (Springer, Berlin) 1991.
[2] Reichl L. E., *A Modern Course in Statistical Physics*, second edition (Wiley, New York) 1998.
[3] Risken H., *The Fokker-Planck Equation*, second edition (Springer-Verlag, Berlin) 1989.
[4] Tsallis C., *Introduction to Nonextensive Statistical Mechanics* (Springer, New York) 2009.
[5] Frank T. D., *Nonlinear Fokker-Planck Equations: Fundamentals and Applications* (Springer, Berlin) 2005.
[6] Shiino M., *J. Math. Phys.*, **42** (2001) 2540.
[7] Kaniadakis G., *Phys. Lett. A*, **288** (2001) 283.
[8] Frank T. D. and Daffertshofer A., *Physica A*, **295** (2001) 455.

[9] Chavanis P. H., *Phys. Rev. E*, **68** (2003) 036108.
[10] Schwämmle V., Nobre F. D. and Curado E. M. F., *Phys. Rev. E*, **76** (2007) 041123.
[11] Schwämmle V., Curado E. M. F. and Nobre F. D., *Eur. Phys. J. B*, **58** (2007) 159.
[12] Nobre F. D., Souza A. M. C. and Curado E. M. F., *Phys. Rev. E*, **86** (2012) 061113.
[13] Curado E. M. F., Souza A. M. C., Nobre F. D. and Andrade R. F. S., *Phys. Rev. E*, **89** (2014) 022117.
[14] Andrade R. F. S., Souza A. M. C., Curado E. M. F. and Nobre F. D., *EPL*, **108** (2014) 20001.
[15] Nobre F. D., Curado E. M. F., Souza A. M. C. and Andrade R. F. S., *Phys. Rev. E*, **91** (2015) 022135.
[16] Ribeiro M. S., Casas G. A. and Nobre F. D., *Phys. Rev. E*, **91** (2015) 012140.
[17] Souza A. M. C., Andrade R. F. S., Nobre F. D. and Curado E. M. F., *Physica A*, **491** (2018) 153.
[18] Lee C.-S., Jankó B., Derényi I. and Barabási A.-L., *Nature*, **400** (1999) 337.
[19] Boghosian B. M., *Phys. Rev. E*, **53** (1996) 4754.
[20] Beck C., *Physica A*, **331** (2004) 173.
[21] Yalcin G. C. and Beck C., *Sci. Rep.*, **8** (2018) 1764.
[22] Khrapak S. A., Ivlev A. V. and Morfill G., *Phys. Rev. E*, **64** (2001) 046403.
[23] Brunner M., Bechinger C., Strepp W., Lobaskin V. and von Grünberg H. H., *Europhys. Lett.*, **58** (2002) 926.
[24] Vaulina O. S., Vladimirov S. V., Petrov O. F. and Fortov V. E., *Phys. Plasmas*, **11** (2004) 3234.
[25] Vaulina O. S., Koss X. G., Khrustalyov Y. V., Petrov O. F. and Fortov V. E., *Phys. Rev. E*, **82** (2010) 056411.
[26] Quarati P. and Scarfone A. M., *Astrophys. J.*, **666** (2007) 1303.
[27] Liu B. and Goree J., *Phys. Rev. Lett.*, **100** (2008) 055003.
[28] Khrapak S. A. and Morfill G. E., *Phys. Rev. Lett.*, **103** (2009) 255003.
[29] Gougam L. A. and Tribeche M., *Phys. Plasmas*, **18** (2011) 062102.
[30] Rios L. A., Galvão R. M. O. and Cirto L., *Phys. Plasmas*, **19** (2012) 034701.
[31] Gougam L. A. and Tribeche M., *Phys. Plasmas*, **19** (2012) 034702.
[32] Jackson J. D., *Classical Electrodynamics*, second edition (John Wiley and Sons, New York) 1975.
[33] Zapperi S., Moreira A. A. and Andrade J. S., *Phys. Rev. Lett.*, **86** (2001) 3622.
[34] Andrade J. S. jr., da Silva G. F. T., Moreira A. A., Nobre F. D. and Curado E. M. F., *Phys. Rev. Lett.*, **105** (2010) 260601.
[35] Ribeiro M. S., Nobre F. D. and Curado E. M. F., *Phys. Rev. E*, **85** (2012) 021146.
[36] Chaikin P. M. and Lubensky T. C., *Principles of Condensed Matter Physicis* (Cambridge University Press, Cambridge) 1995.
[37] Matias A. F. V., Shinbrot T. and Araujo N. A. M., *Phys. Rev. E*, **98** (2018) 062903.